Optimal Control Techniques for Assessing Feasibility and Defining Subsystem Level Requirements: An Automotive Case Study

Ilya V. Kolmanovsky, *Member, IEEE,* and Anna G. Stefanopoulou, *Member, IEEE*

***Abstract*—The use of models is widespread in automotive industry in the preliminary feasibility assessment of novel powertrains, determination of system configuration and subsystem requirements, and operating strategy. Although optimal control problems arise naturally within this context when faced with analysis of transient performance requirements, they are rarely treated other than by simulations. The objective of this paper is to illustrate how optimal control problems of this kind arise and can be solved numerically using optimal control techniques. We also demonstrate an array of meaningful conclusions that can be generated from such an optimal control study. The case study treated in the paper deals with a turbocharger power assist system (TPAS). The extent to which this system can reduce the diesel engine turbo-lag is determined via the numerical solution of a minimum-time optimal control problem.**

***Index Terms*—Automotive applications, optimal control, optimization.**

Nomenclature of Main Engine Variables

p_1	pressure in intake manifold
p_2	pressure in exhaust manifold
p_{amb}	ambient pressure
ρ_1	density in intake manifold
ρ_2	density in exhaust manifold
N_{tc}	turbocharger speed
N_e	engine speed
N_v	vehicle speed
P_{em}	TPAS power applied to the turbo shaft
E_{em}	TPAS energy consumption
P_t	power generated by the turbine
P_c	power consumed by compressor
TQ_e	engine torque
TQ_l	load torque on the crankshaft
W_f	engine fueling rate
W_{1e}	mass flow rate into the engine cylinders
W_{c1}	mass flow rate through the compressor
W_{e2}	mass flow rate from the engine into the exhaust manifold
W_{2t}	mass flow rate through the turbine
(A/F)	engine air-to-fuel ratio
T_1	temperature in intake manifold
T_{c1}	temperature of gas flowing through the compressor
T_{e2}	temperature of gas flowing from the engine into the exhaust manifold
T_2	exhaust manifold temperature
η_{vol}	engine volumetric efficiency
η_t	turbine isentropic efficiency
η_c	compressor isentropic efficiency
η_m	turbocharger mechanical efficiency
q_m	average TPAS motoring efficiency
q_g	average TPAS regenerating efficiency
V_1	intake manifold volume
V_2	exhaust manifold volume
V_d	engine displacement volume
I_v	total vehicle inertia reflected to the engine shaft
I_{tc}	turbocharger shaft rotational inertia
c_p	specific heat at constant pressure
c_v	specific heat at constant volume
γ	specific heat ratio (constant)
R	specific heat difference.

Manuscript received February 23, 2000; revised September 1, 2000. Manuscript received in final form November 21, 2000. Recommended by Associate Editor J. Chiasson.

I. V. Kolmanovsky is with the Ford Research Laboratory, Dearborn, MI 48121-2053 USA (e-mail: ikolmano@ford.com).

A. G. Stefanopoulou is with the University of Michigan, Ann Arbor, MI 48109 USA (e-mail: annastef@umich.edu).

Publisher Item Identifier S 1063-6536(01)03361-9.

I. Introduction

MODERN automotive powertrains have to meet a multiplicity of requirements. Some of these requirements stem from the environmental regulations, others reflect fuel economy or customer perception of subjective characteristics such as "fun to drive." Typically, meeting these diverse requirements involves a combination of hardware and control solutions. In the business environment that calls for aggressive reduction in the time-to-market, the importance of making the right decisions about hardware configuration, subsystem level requirements, and operating strategy early on in the design stage increases dramatically. This trend forces more reliance on the simulation models in the early phase of developing a new automotive system especially when studying its feasibility with regards to meeting the diverse requirements. When faced with transient performance objectives, the determination of subsystem level requirements and the study of the system feasibility reduces frequently to solving an optimal control problem. Because the simulation models are often high order and complex, the analytical solution is typically ruled out and numerical methods have to be used. Given the importance of the problem, one would expect that the optimal control methods would find widespread use but judging by the published literature, this is not the case.

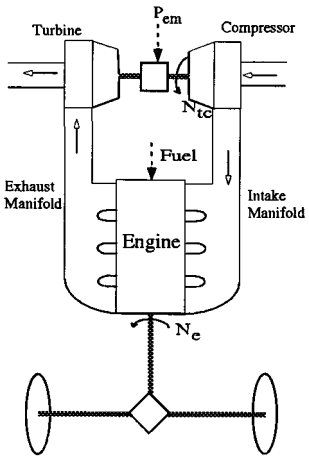

Fig. 1. Schematic representation of a diesel engine with a turbocharger power assist system.

The objective of this paper is to demonstrate how the optimal control problems arise in the process of new powertrain assessment and how these problems can be solved numerically. Their solution can yield meaningful conclusions in the following areas:

- cost-benefit tradeoff;
- subsystem level requirements;
- control strategy implications.

The case study that we consider is concerned with a turbocharger power assist system (TPAS) for a turbocharged diesel engine. We now review the basic context in which this problem appears.

One of the key tradeoffs in the operation of passenger car turbocharged diesel engines is between the smoke/particulate emissions and acceleration performance. To prevent visible smoke emissions from the engine the air-to-fuel ratio should be maintained at a sufficiently high value. The intake air dynamics in a turbocharged diesel engine [see Fig. 1] are driven by the turbocharger dynamics and by the intake manifold and exhaust manifold filling dynamics. The engine exhaust gas passes through the turbine, spinning up the turbine wheel, and this rotation is transferred to the compressor wheel which is connected to the turbine wheel rigidly by a shaft. The compressor wheel imparts the kinetic energy to the intake air that is converted into the increase in air pressure and density in the compressor diffuser. The fuel is injected directly into the combustion chamber. Due to the air-to-fuel ratio constraint, the rate of increase in the fueling rate and, hence, engine torque, is limited by the rate with which the airflow can be increased. Hence, the turbocharger has to spin up and the intake manifold pressure has to rise before a substantial increase in the engine torque output can occur. This is the main cause of the sluggish response of a diesel engine to a driver's pedal tip-in also known as the turbo-lag.

An important objective in diesel engine development is to improve its acceleration performance without relaxing the zero visible smoke constraint. Ultimately, the goal is to achieve the so called spark ignition engine "transparency" when the driver should not notice any significant differences in the acceleration performance when driving a diesel-powered vehicle. This goal can be addressed via a combination of hardware and control solutions. From the hardware standpoint, it is natural to investigate advanced turbocharger concepts where ancillary means are provided to spin up the turbocharger for faster increase in the airflow. A possible hardware solution is a turbocharger power assist system (TPAS). This can be any device capable of supplying torque to the turbocharger shaft in the motoring mode and absorbing power from the turbocharger shaft and storing it when engaged in the regenerative mode. (See Fig. 1.) The TPAS can be engaged at tip-ins to rapidly raise the turbocharger speed and fresh air delivery to the engine, thereby, increasing engine torque output with no deleterious effect on smoke. At higher engine speeds and loads, the TPAS, engaged in a regenerative mode, can play the role of a conventional wastegate. By applying a negative torque to the turbocharger shaft during the regenerative mode the TPAS can prevent the turbocharger shaft from overspinning. It can also keep the fuel consumption low which, otherwise, may be negatively affected by high pumping losses associated with high exhaust manifold pressure. At the same time while "braking" the turbocharger the TPAS can store the energy absorbed from the turbocharger shaft for the future use. This energy would be wasted in a conventional engine since a portion of the exhaust gas bypasses the turbocharger when the wastegate opens. The implementation of TPAS based on the electric motor and battery technology is currently under intensive development, see [11], [3], [5].

To justify the cost associated with the device an assessment of the benefits is needed. In particular, we need to determine to which extent we can reduce the turbo-lag and thus improve acceleration performance. We concentrate on fixed gear acceleration tests for the TPAS performance assessment because they provide insights into important driveability characteristics such as car "highway passing" performance or "launch" performance from idle [10]. These tests are also convenient because they do not require the simultaneous optimization of the gear ratio trajectory thereby leading to substantial complexity reduction of the optimal control problem. We concentrate on these fixed gear acceleration tests and neglect wheel slip and clutch/driveline dynamics in the TPAS performance assessment.

It is important to make the right decision about the degree of detail to be included in the models and constraints used in the initial assessment phase. Very detailed models may be difficult to treat numerically and may obscure trends and conclusions. On the other hand, insufficient modeling details or unrealistic constraints may lead to incorrect conclusions. Making the right tradeoff in this situation depends largely on experience of an application engineer.

Our analysis is based on a mean-value model of the diesel engine and a generic power addition-energy storage representation for the TPAS. The maximum power that can be delivered or absorbed by the TPAS is limited. To avoid depleting the energy storage an additional constraint is imposed, namely, the net TPAS energy consumption during the acceleration to a desired final vehicle velocity should be nonpositive. Thus all the energy supplied by the TPAS to the turbocharger shaft must be regenerated by the end of the acceleration interval.

This paper is organized as follows. In Section II we describe the model used in this study. We then carefully formulate the

turbo-lag reduction problem as a minimum time optimal control problem and describe a numerical approach to solving it in Section III. Analysis of the sensitivity of the conclusions to parameter changes and additional constraints is the subject of Section IV. The effects of turbocharger rotational inertia changes, motoring and regenerating efficiencies, as well as maximum torque limits are studied within the same numerical optimal control framework. An on-line controller implementation motivated by the optimized trajectory patterns is presented in Section V. The conclusions can be found in Section VI.

II. Preliminaries

A. Powertrain Model

The study is based on a model of a medium-size passenger car with a high-speed diesel engine equipped with TPAS. The model is based on the standard representations for the gas filling dynamics in the manifolds of the engine, turbocharger dynamics, and vehicle longitudinal dynamics. The specific subsystem representations and modeling assumptions for turbocharged diesel engines are borrowed from [6], [7]. Here we assume zero exhaust gas recirculation because EGR is typically disabled during aggressive acceleration phases that are of most interest in this paper.

The power supplied by the TPAS to the turbocharger shaft, P_{em}, is a control input to the system

$$u = P_{em}. \tag{1}$$

The power is applied to the turbocharger shaft if u is positive and it is absorbed from the turbocharger shaft if u is negative. Applying power balance to the turbocharger shaft, we obtain

$$(I_{tc}N_{tc})\frac{d}{dt}N_{tc} = \eta_m P_t - P_c + P_{em}. \tag{2}$$

Here, N_{tc} is the turbocharger rotational speed, I_{tc} is the turbocharger shaft rotational inertia, P_t is the power generated by the turbine, P_c is the power consumed by the compressor and η_m is the turbocharger mechanical efficiency. The turbine and compressor powers are calculated based on the first law of thermodynamics applied to the control volumes of the turbine and of the compressor

$$P_t = W_{2t}c_p\eta_t\eta_m T_2\left(1 - \left(\frac{p_{amb}}{p_2}\right)^{(\gamma-1/\gamma)}\right) \tag{3}$$

$$P_c = W_{c1}c_p\frac{1}{\eta_c}T_{amb}\left(\left(\frac{p_1}{p_{amb}}\right)^{(\gamma-1/\gamma)} - 1\right). \tag{4}$$

Here, W_{2t} is the mass flow rate of gas through the turbine, W_{c1} is the mass flow rate through the compressor, p_1 is the pressure in the intake manifold, p_2 is the pressure in the exhaust manifold, T_1 is the temperature in the intake manifold, T_2 is the temperature in the exhaust manifold, p_{amb} is the ambient pressure, T_{amb} is the ambient temperature, c_p is the specific heat capacity at constant pressure, η_t is the turbine isentropic efficiency, η_c is the compressor isentropic efficiency and γ is a ratio of specific heats of the gas. The efficiencies and mass flow rates through the turbine and the compressor are calculated from nonlinear regressions

$$\begin{bmatrix} \dfrac{W_{2t}p_2}{\sqrt{T_2}} \\ \eta_t \end{bmatrix} = f_t\left(\frac{p_{amb}}{p_2}, \frac{N_{tc}}{\sqrt{T_2}}\right) \tag{5}$$

$$\begin{bmatrix} \dfrac{W_{c1}p_{amb}}{\sqrt{T_{amb}}} \\ \eta_c \end{bmatrix} = f_c\left(\frac{p_1}{p_{amb}}, \frac{N_{tc}}{\sqrt{T_{amb}}}\right). \tag{6}$$

The supplemental power P_{em} directly affects the time rate of change of turbocharger speed which, in turn, affects the flows through the compressor and the turbine and the pressures in the intake and exhaust manifolds. The dynamics of gas density (ρ_1) and pressure (p_1) in the intake manifold are described by the following equations that are obtained from the mass balance and enthalpy balance

$$\begin{aligned} \frac{d}{dt}\rho_1 &= \frac{1}{V_1}(W_{c1} - W_{1e}), \\ \frac{d}{dt}p_1 &= \frac{\gamma R}{V_1}(W_{c1}T_{c1} - W_{1e}T_1). \end{aligned} \tag{7}$$

Here, W_{1e} is the total flow mass flow rate of gas from the intake manifold into the engine (mean value, i.e., averaged over an engine cycle). V_1 is the intake manifold volume, T_{c1} is the temperature of gas at the compressor outlet calculated from

$$T_{c1} = \frac{1}{\eta_c}T_{amb}\left(\left(\frac{p_1}{p_{amb}}\right)^{(\gamma-1/\gamma)}\right) \tag{8}$$

and T_1 is the temperature of the gas in the intake manifold calculated using the ideal gas law, $T_1 = p_1/(R\rho_1)$, where R is the difference of the specific heats. The exhaust manifold pressure p_2 and density ρ_2 are described by similar two equations

$$\begin{aligned} \frac{d}{dt}\rho_2 &= \frac{1}{V_2}(W_{e2} - W_{2t}), \\ \frac{d}{dt}p_2 &= \frac{\gamma R}{V_2}(W_{e2}T_{e2} - W_{2t}T_2) \end{aligned} \tag{9}$$

where

- W_{2t} mass flow rate through the turbine;
- W_{e2} mass flow rate out of the engine cylinders into the exhaust manifold (mean-value, i.e., averaged over an engine cycle);
- V_2 exhaust manifold volume.

Neglecting engine cycle delays

$$W_{e2} = W_{1e} + W_f \tag{10}$$

where W_f is the cycle averaged fueling rate. The engine outlet temperature T_{e2} is calculated from a regression of the form

$$T_{e2} = T_1 + f_{e2}(W_f, W_{1e}, N_e). \tag{11}$$

Note that this expression accounts for heat losses in the exhaust manifold in steady-state because it is typically developed on the basis of engine mapping data with the heat losses already factored in. For the fully warmed up operation we have found that the simplified adiabatic approximation (9) of the exhaust manifold dynamics combined with (11) provides a good accuracy

in predicting pressures, flows and turbocharger speed, see, for example, [8].

The total engine intake mass flow rate is given by

$$W_{1e} = \eta_{vol}\rho_1 V_d \frac{N_e}{120} \tag{12}$$

where V_d is the engine displacement volume, N_e is the engine speed, and the volumetric efficiency η_{vol} is determined from a regression of the form

$$\eta_{vol} = \eta_{vol}(p_1, p_2, N_e, T_1, T_2). \tag{13}$$

The dynamics of the engine speed N_e follow from the torque balance on the crankshaft

$$I_v \frac{d}{dt} N_e = TQ_e - TQ_l. \tag{14}$$

Here, I_v is the total vehicle inertia reflected to the engine shaft, TQ_e is the engine brake torque and TQ_l is the load torque, calculated from the aerodynamic and rolling resistance forces on the vehicle and known (fixed) gear ratio. With a fixed injection timing strategy the engine brake torque TQ_e is calculated form a regression of the form

$$TQ_e = TQ_e(W_f, N_e, p_1, p_2, (A/F)) \tag{15}$$

where $(A/F) = W_{1e}/W_f$ is the in-cylinder air-to-fuel ratio. The torque dependence on the pressures is primarily due to pumping losses. Indeed, the engine can draw air easier from a manifold at a higher pressure and it can exhaust the air easier against a lower exhaust manifold pressure.

We denote by N_v the vehicle speed. We assumed that the gear ratio is fixed, thus, N_v is proportional to N_e.

As can be seen from the model, the TPAS affects the engine operation in a profound way. Through its effect on the turbocharger rotational speed, it affects the mass flow rates of gas through the compressor and through the turbine. These flows, in turn, affect the intake and exhaust manifold pressures and, therefore, engine intake airflow W_{1e}, volumetric efficiency η_{vol} and the engine brake torque TQ_e. As we will see in the following section the engine fueling rate W_f cannot rise faster than the airflow W_{1e} during the aggressive acceleration phases and this is, actually, the main reason why the turbocharger and the TPAS have a profound effect on the engine torque response.

The TPAS model is a rather generic energy addition/storage mechanism

$$\dot{E}_{em} = P_{em}. \tag{16}$$

The state of the overall system is a vector

$$x = [\rho_1 \quad p_1 \quad \rho_2 \quad p_2 \quad N_{tc} \quad N_e \quad E_{em}]. \tag{17}$$

We also let

$$r \triangleq W_f. \tag{18}$$

Then, the engine and vehicle dynamics comprise a nonlinear control system of the general form

$$\frac{d}{dt} x = f(x, u, r). \tag{19}$$

B. Smoke-Limited Acceleration

The generation of visible smoke can be avoided if the air-to-fuel ratio is kept sufficiently high both in transients and in steady state, i.e.,

$$(A/F)(t) = \frac{W_{1e}(t)}{W_f(t)} \geq (A/F)_{\min} \tag{20}$$

where $(A/F)_{\min}$ is the minimum value of the air-to-fuel ratio. Consequently, the fueling rate in the engine is limited by the control system so that if $W_{f,req}$ is the desired fueling rate (requested by the driver via pedal depression) then the actual fueling rate is

$$W_f = \min\left\{\frac{W_{1e}}{(A/F)_{\min}}, W_{f,req}\right\}. \tag{21}$$

If the driver's request is to accelerate as fast as possible, the fueling limiter is active and

$$r(t) = W_f(t) = \frac{W_{1e}(t)}{(A/F)_{\min}}. \tag{22}$$

This expression shows that during aggressive acceleration the engine fueling rate cannot increase faster than the airflow and this is what causes the sluggish engine torque response, or the turbo-lag. In the simulations and optimization we assumed a conservative value of $(A/F)_{\min} = 25$.

We let

$$r^*(x) \triangleq \frac{W_{1e}}{(A/F)_{\min}} \tag{23}$$

and

$$F(x, u) \triangleq f(x, u, r^*(x)). \tag{24}$$

III. Optimal Acceleration with TPAS

A. Minimum-Time Problem Formulation

The objective is to determine the minimum time, T, for a fixed gear acceleration to a specified final vehicle speed, N_v^d. The acceleration proceeds with the fueling limiter active. The maximum power that the TPAS can deliver or absorb is constrained as

$$|P_{em}| = |u(t)| \leq u_{\max} \tag{25}$$

where $u_{\max}$ is the limit. The total energy expenditure by the TPAS over the acceleration interval must be less than zero. This is a rather conservative requirement but it is needed to ensure that the energy storage is never depleted. Since the gear is fixed the constraint on the final vehicle speed, $N_v(T)$, is really a constraint on the final engine speed, $N_e(T)$, to be equal to the desired value, N_e^d. Formally, the problem is formulated as

$$\text{Minimize} \quad J(u, T) \triangleq T \quad \text{subject to} \tag{26}$$

$$|u(t)| = |P_{em}(t)| \leq u_{\max}, \qquad 0 \leq t \leq T \tag{27}$$

$$\int_0^T u(t)\, dt = E_{em}(T) - E_{em}(0) \leq 0 \tag{28}$$

$$g(u, T) \triangleq N_e(T) - N_e^d = 0 \tag{29}$$

$$\dot{x} = F(x(t), u(t)), \qquad x(0) = x^0. \tag{30}$$

Here, x^0 is the initial equilibrium, corresponding to either the engine in neutral idle or to steady highway cruising conditions.

B. Necessary Conditions for Optimality

The necessary conditions for optimality, in the form of Pontryagin's maximum principle [2], are useful in providing insight about the optimal solution. The Hamiltonian for this problem has the form

$$H(x, u, p) = p_0 + p^T F(x, u) \tag{31}$$

where p is the vector of the adjoint variables that has the same dimension as x. The optimal solution x^*, u^*, T^* satisfies the adjoint differential equation

$$\dot{p} = -\left(\frac{\partial H}{\partial x}\right)^T \tag{32}$$

for some trajectory p^* and some value of $p_0 \in \{0, 1\}$. Note that the final value of the adjoint variables, $p^*(T)$, is constrained through the transversality conditions [2]. If we write out all the terms in H that depend on u we obtain

$$\left(\frac{p_5(t)}{I_{tc}N_{tc}(t)} + p_7(t)\right) u(t). \tag{33}$$

The pointwise minimization of the Hamiltonian with respect to u then yields that the optimal control is of bang-bang type, $u^*(t) = u_{\max}$ or $u^*(t) = -u_{\max}$ as long as the expression in the brackets is nonzero. If the expression in the brackets is zero then the minimization of H does not yield any information about $u^*(t)$ and the problem is singular. Since f does not depend on $x_7 = E_{em}$, the optimal trajectory of the adjoint variable $p_7(t)$, $p_7^*(t)$, is a constant and does not depend on t. Consequently, within any time interval $\sigma_1 \le t \le \sigma_2$, where $-u_{\max} < u^*(\sigma) < u_{\max}$, it must be true that

$$\frac{p_5^*(t)}{N_{tc}^*(t)} \equiv c \tag{34}$$

where c is a constant (the same for all such intervals).

The existence of singular optimal trajectories in the minimum time optimal control problems is not unusual. Specific examples can be found in [1], [2], [9]. In this case the optimal control contains the so called singular arcs that are frequently *not* of bang-bang character. More complex, higher order necessary conditions for optimality, may be applicable in this case, see, e.g., [1, pp. 351–359].

C. Numerical Optimization Procedure

It is clear that the optimal control problem cannot be treated analytically. We, thus, take a numerical approach. Since the solution of an affine in control minimum time problem is "most likely" of bang-bang character the traditional numerical procedure would be to seek u in the class of piecewise constant functions and optimize the location and the number of the switching points where the control switches between $-u_{\max}$ and $u_{\max}$. This approach, however, may miss a singular solution if, indeed, this solution happens to be the true optimum. Hence, a more flexible procedure that is capable of approximating both regular and singular solutions is needed. The procedure used in our paper is, indeed, of this type. It relies on the parameterization of the control input using linear B-splines and it optimizes the coefficients in this parameterization. The idea of directly parameterizing the input is fairly standard in the optimal control literature, see, e.g., [4], [1]. A more detailed description of the procedure that we used follows.

As a first step, it is actually more convenient for the numerical treatment to recast the problem as a fixed-time problem. This is done by rescaling time

$$\sigma = \frac{t}{T}, \qquad 0 \le \sigma \le 1. \tag{35}$$

Then, (19) becomes

$$\frac{dx}{d\sigma} = TF(x, u), \qquad x(0) = x^0, \quad 0 \le \sigma \le 1. \tag{36}$$

Note that T is now a parameter, scaling the dynamics. We need to optimize T and the control input trajectory $u(\sigma)$, $0 \le \sigma \le 1$, so that T is a minimum and the constraints

$$|u(\sigma)| \le u_{\max}, \qquad 0 \le \sigma \le 1 \tag{37}$$

$$\int_0^1 u(\sigma)\, d\sigma \le 0 \tag{38}$$

$$g(u, T) = 0 \tag{39}$$

$$\frac{dx}{d\sigma} = TF(x, u), \qquad x(0) = x^0, \quad 0 \le \sigma \le 1 \tag{40}$$

are satisfied.

The linear B-splines used in the parameterization of u are defined as follows. For an integer k, we let

$$\phi_0(\Delta;\, \sigma) = \begin{cases} 1 - \dfrac{|\sigma|}{\Delta}, & |\sigma| \le \Delta, \\ 0, & \text{otherwise} \end{cases} \tag{41}$$

$$\phi_k(\Delta;\, \sigma) = \phi_0(\Delta;\, \sigma - k\Delta). \tag{42}$$

Then, u is parameterized as a weighted sum of the B-splines with unknown weights α_i

$$u(\sigma) = \sum_{i=0}^{n} \alpha_i \phi_i(\Delta;\, \sigma), \qquad 0 \le \sigma \le 1 \tag{43}$$

where $\Delta > 0$ and n is a positive integer such as $1 = n \cdot \Delta$.

Note that the coefficients, α_i, $i = 0, \ldots, n$, in this parameterization are precisely the values $u(\Delta \cdot i)$, $i = 0, \ldots, n$. This property facilitates the development of iterative algorithms where n, Δ can be changed (e.g., to obtain better accuracy) and the solution obtained in the previous iteration is used as an initial guess for the next iteration. In this situation, linear B-splines allow to rapidly move from coefficients of the old parameterization to the coefficients of the new parameterization. Furthermore, to simulate the model in Matlab/Simulink it is only necessary to supply the values of α_i, $i = 0, \ldots, n$, as a vector while the interpolation (43) is done automatically.

The numerical optimization was performed using function `constr.m` of the Matlab 5.2 optimization toolbox which is based on a sequential quadratic programming (SQP) algorithm for constrained minimization. To handle large values of n we relied on explicit gradient computation through the backward integration of the adjoint equations. See Appendix A. For large n, explicit gradient calculation that takes advantage of the sequential nature of system dynamics is more efficient than the use of a center-difference formula-like approximation (see [4]). We found that the explicit gradient computation was essential to handle numerically large values of n. The linearized equations of the diesel engine and vehicle dynamics required to formulate the adjoint equations have been derived symbolically from the nonlinear model equations with an automatic differentiator that we developed. The automatic differentiator is based on Matlab Symbolic Toolbox, it takes as an input the S-function of the

model and generates a ready-to-simulate S-function of the adjoint system.

D. Numerical Optimization Results

We apply the optimization procedure to two scenarios of acceleration requests. The first scenario addresses the "launch performance" of the vehicle while the second scenario addresses the "highway passing" performance of the vehicle.

The optimized performance and trajectories are compared to those of a "conventional" vehicle. The "conventional" vehicle represents in this work the same vehicle model but with the TPAS turned off, i.e., when $u = P_{em} \equiv 0$. The "conventional vehicle" represents the simplest baseline for evaluating the benefits of adding supplemental power to the turbocharger shaft. To fully justify the cost-benefit tradeoff for the TPAS, it is also necessary to compare its performance benefits with performance benefits that can be provided by other advanced boosting technology. For example, a variable geometry turbocharger (VGT) with actuated guide vanes at the turbine stator can be used for turbo-lag reduction. To evaluate the system with VGT one would also have to optimize the trajectory of the turbine guide vanes during the acceleration. This is more complex but it can be accomplished using the same optimal control techniques described in this paper. See also [8], where these optimal control techniques are utilized for determining the optimal pattern of coordinating EGR and VGT actuators.

Since for the first and third gear acceleration tests the intake and exhaust manifold pressures remain relatively low, we make an assumption that the wastegate of the conventional engine remains closed.

Throughout, we refer to the performance and trajectories as "optimized" rather than "optimal." This is a reflection of the fact that we used a numerical and an approximate method to solve the optimal control problem. We expect that the true optimal solution is close to the optimized one.

The "launch performance" is evaluated by considering a first gear acceleration. In this scenario the vehicle starts from idle and accelerates to 40 km/h. We use $n = 23$ in the parameterization of u with linear B-splines. Several optimization runs, initialized with different sets of initial values for α_i, $i = 1, \ldots, n$ and T, converged to trajectories shown in Figs. 2 and 3. The circles superimposed on the $u(t) = P_{em}(t)$ trajectory indicate the values of α_i, $i = 0, \ldots, n$. The results are also summarized in Table I, where "energy spent" is equal to the total chemical energy released by burning fuel since the total energy spent by the TPAS is zero. The optimized operation of the TPAS achieves approximately 15.1% improvement in acceleration time and results in 2.1% less fuel consumption as compared to the conventional vehicle. The P_{em} trajectory in Fig. 2 is of bang-bang character, as may be expected from the analysis of the necessary conditions in Section III-B. The supplemental power is applied in the initial phase of the acceleration to rapidly spin up the turbocharger and is regenerated in the final phase of the acceleration. From Fig. 3 we observe that operating the TPAS in the motoring mode results in a smaller difference between the exhaust manifold pressure and the intake manifold pressure, $p_2 - p_1$, than in the conventional vehicle case. This corresponds to, initially, lower pumping losses and contributes to higher engine torque output

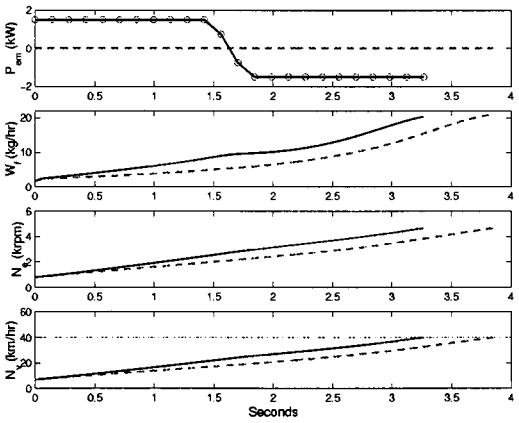

Fig. 2. Comparison of TPAS (solid) and conventional vehicle (dashed) for the first gear acceleration. Trajectories of P_{em}, W_f, N_e and N_v.

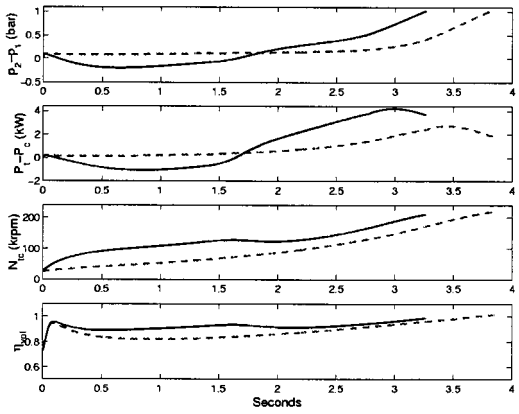

Fig. 3. Comparison of TPAS (solid) and conventional vehicle (dashed) for the first gear acceleration. Trajectories of $p_2 - p_1$, $P_t - P_c$, N_{tc}, η_{vol}.

TABLE I
THE ACCELERATION TIME, FUEL CONSUMPTION AND TOTAL CHEMICAL AND SUPPLEMENTAL (FUEL+TPAS) ENERGY CONSUMPTION FOR THE FIRST GEAR ACCELERATION

	Time (sec)	Fuel (g)	Energy (MJ)
TPAS Vehicle	3.27	8.55	0.363
Conv. Vehicle	3.85	8.73	0.371

and faster acceleration. The reduction in pumping losses is particularly beneficial at low engine speeds and loads, where the engine is rather inefficient. Thus, it is no surprise that the total fuel consumption for the vehicle with the TPAS is slightly lower than for the conventional vehicle. Finally, the increase in the volumetric efficiency at the beginning of the acceleration is also beneficial as even more fuel can be injected to enable faster vehicle acceleration.

Consider now the "highway passing" performance. It is evaluated using an acceleration scenario in the third gear, where the vehicle starts from a steady-state cruise condition at 40 km/h and accelerates to 90 km/h. Figs. 4 and 5 and Table II summarize the results. The acceleration time of the vehicle with the TPAS is 8.44% better than the conventional vehicle while the fuel consumption is essentially the same in both cases. The optimal control is at the extreme values only in the very initial and in the very

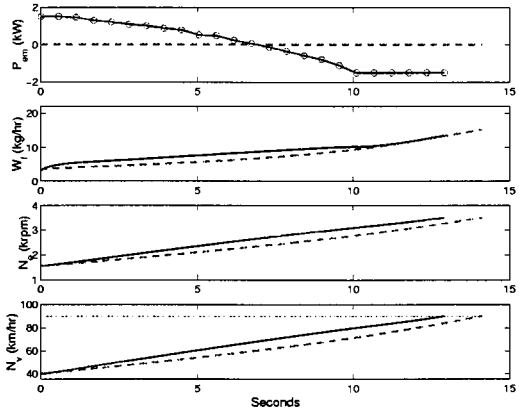

Fig. 4. Comparison of TPAS (solid) and conventional vehicle (dashed) for the third gear acceleration. Trajectories of P_{em}, W_f, N_e and N_v.

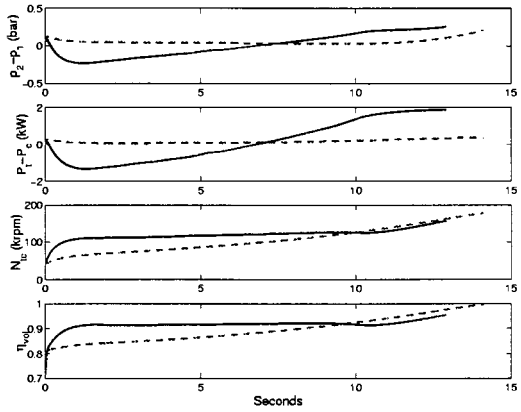

Fig. 5. Comparison of TPAS (solid) and conventional vehicle (dashed) for the third gear acceleration. Trajectories of $p_2 - p_1$, $P_t - P_c$, N_{tc}, η_{vol}.

TABLE II
THE ACCELERATION TIME, FUEL CONSUMPTION AND TOTAL CHEMICAL AND SUPPLEMENTAL (FUEL+TPAS) ENERGY CONSUMPTION FOR THE THIRD GEAR ACCELERATION

	Time (sec)	Fuel (g)	Energy (MJ)
TPAS Vehicle	12.91	30.27	1.286
Conv. Vehicle	14.10	30.31	1.288

final phases of the acceleration. The limits are not active in-between suggesting that the optimal solution contains a singular arc. To check this hypothesis the numerical optimization was repeated for several random initializations and varying number of knots. The trajectories have always converged to trajectories shown in Figs. 4 and 5. From physical reasons we expect that if the optimal control is of bang-bang character without the singular arc then it involves just one switch. Hence, we numerically searched for an optimal solution in the class of bang-bang controls with a single switch. The solution found in this class yielded larger minimum time than for the trajectories shown in Figs. 4 and 5. Thus it appears that a solution with the singular arc is optimal.

IV. SENSITIVITY

The above conclusions may already serve as a basis for an initial decision on whether the cost of the TPAS can be justified on the basis of the performance benefits that this hardware component can provide. Specifically, the analysis has shown that sizable improvements in the acceleration time can be attained even if the net energy consumption by the TPAS during the acceleration interval is zero. It is especially important to note that the initial acceleration performance is substantially improved. The improvements in fuel consumption are rather small on the percentage basis but the important conclusion is that the fuel consumption does not deteriorate during the more aggressive acceleration with the TPAS. The optimization analysis also uncovered the physical reasons behind these performance benefits and enabled us to build some intuition about the device operation. The analysis also indicated how the hardware component should be operated to achieve maximum performance benefits.

Before a more definite recommendation can be made, however, we need to determine the sensitivity of our conclusions to the assumptions that we made. This sensitivity analysis will also lead to the specification of subsystem level requirements necessary to achieve the desired performance targets. Once these specifications have been made an engineer may either attempt to develop an appropriate hardware component in-house or work to identify an appropriate supplier.

For our case study the four critical parameters are 1) the inertia of the rotating parts of the turbocharger and TPAS; 2) the maximum power limit; 3) limits on the torque that the TPAS can deliver or absorb; and 4) the motoring and regenerating efficiencies. Since the TPAS would normally be integrated into the turbocharger housing, the inertia of the rotating parts may change as compared to the turbocharger of the conventional vehicle. The increase in inertia may be detrimental to the acceleration performance and hence this effect has to be considered in detail and quantified. The maximum power limit in 2) and the maximum torque limits in 3) are, of course, important subsystem level requirements that need to be identified. Note that typical electric motors exhibit both power limits and torque limits. The torque limits may become active at low rotational speeds while the power limits would, typically, become active at high rotational speeds. Finally, the motoring and regenerating efficiencies in 4) characterize the level of losses involved into the energy transfer and energy storage within the TPAS. Once the acceptable range of motoring and regenerating efficiencies that allow to meet the performance targets are identified they can be communicated to the component manufacturers or used to select an appropriate product from several offerings.

Note that the sensitivity analysis requires solving multiple optimal control problems. Hence, it is critical that the numerical procedure be fast and efficient and this is why the attention to the details of the numerical implementation is very important.

A. Effect of Changing Rotational Inertia

The minimum time to accelerate from idle to 40 km/h in the first gear was determined for different values of the turbocharger rotational inertia. The maximum TPAS power was constrained in magnitude to 1.5 kW. The minimum time as a function of the ratio of the inertia to its nominal value (turbocharger inertia scale factor) is plotted in Fig. 6. We see that the inertia has to increase at least 2.5 times as compared to the conventional vehicle

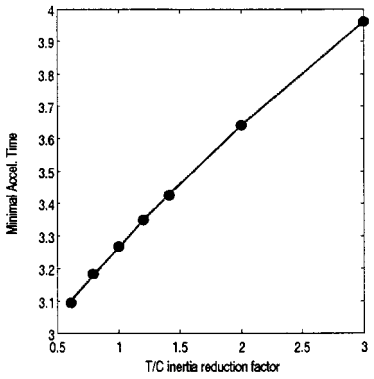

Fig. 6. The minimum acceleration time as a function of the turbocharger inertia scale factor for the first gear acceleration to 40 km/h.

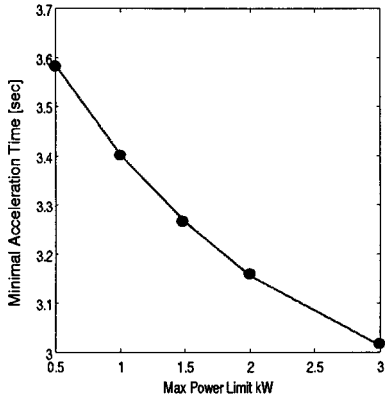

Fig. 7. The minimum acceleration time as a function of the maximum power limit for the first gear acceleration to 40 km/h.

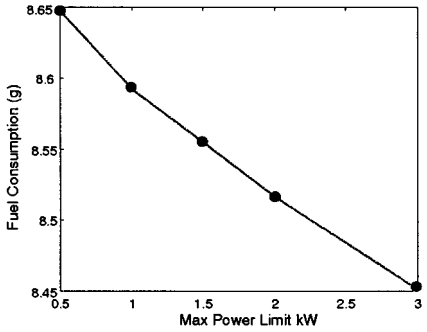

Fig. 8. The fuel consumption as a function of the maximum power limit for the first gear acceleration to 40 km/h.

before the benefits of the TPAS in terms of turbo-lag reduction disappear.

B. Effect of Changing Maximum Power Limit

We consider the effect of varying the maximum power limit, $u_{\max}$, away from the nominal value (1.5 kW). The minimum acceleration time as a function of the maximum power limit for the first gear acceleration to 40 km/h is shown in Fig. 7. Increasing the maximum power limit decreases the minimum acceleration time. Increasing the maximum power limit has a beneficial effect on the fuel consumption, see Fig. 8. Note that the total energy expenditure by the TPAS is zero for all of these values of the maximum power limit.

C. Effect of Changing Maximum Torque Limit

Typical electric motors exhibit both power limits and torque limits with torque limits predominantly active at low rotational speeds and power limits predominantly active at high rotational speeds. If τ_{em} denotes the torque generated or absorbed by the TPAS then the constraint takes the form

$$|\tau_{em}| \leq \tau_{\max} \tag{44}$$

where $\tau_{\max}$ is the limit. The torque constraint can be restated in terms of a state-dependent constraint on P_{em}:

$$|u(t)| \leq \tau_{\max} \cdot N_{tc}(t) \cdot \frac{\pi}{30}. \tag{45}$$

Here the factor $\pi/30$ is used for unit conversion, assuming that N_{tc} is measured in r/min, τ in Nm, and u in W.

To handle the constraint (45), we use an iterative procedure. On the kth step of this procedure we obtain the trajectory of the turbocharger rotational speed, $N_{tc}^k(\sigma)$, $0 \leq \sigma \leq 1$, corresponding to some control $u^k(\sigma) = P_{em}^k(\sigma)$, $0 \leq \sigma \leq T$. Let σ_i^k denote the ith knot in the B-spline parameterization of $u^k(\sigma)$ so that

$$u^k(\sigma_i^k) = \alpha_i^k, \qquad i = 1, \ldots, n. \tag{46}$$

Then, on the $(k+1)$th step the optimization is performed over the values of α_i^{k+1}, subject to an additional constraint of the form

$$|\alpha_i^{k+1}| \leq \tau_{\max} \cdot N_{tc}^k(\sigma_i^{k+1}) \cdot \frac{\pi}{30}, \qquad i = 1, \ldots, n. \tag{47}$$

TABLE III
THE ACCELERATION TIME, FUEL CONSUMPTION AND TOTAL CHEMICAL AND SUPPLEMENTAL (FUEL+TPAS) ENERGY CONSUMPTION FOR THE FIRST GEAR ACCELERATION

	Time (sec)	Fuel (g)	Energy (MJ)
TPAS Vehicle	3.31	8.53	0.363
Conv. Vehicle	3.85	8.73	0.371

As a result, we generate the new control trajectory, u^{k+1}. Then k is incremented and the procedure is repeated. As we iteratively increase k, we intuitively expect the solution to approach the optimal solution. For the application here this approach was used and has been shown to work well. The formal statement of conditions under which this convergence takes place is left to future publications.

The optimization was completed under a $\tau_{\max} = 0.15$ Nm maximum torque limit, in addition, to 1.5 kW maximum power limit and net TPAS energy consumption constrained to be less than zero. The results for the acceleration in the first gear to 40 km/h are summarized in Table III. As compared to the case of power limit only the minimum acceleration time has increased but only slightly. As compared to the conventional vehicle, the improvement in the acceleration time is approximately 13.88%, and the improvement in fuel consumption is approximately 2.28%. The optimized trajectories are shown in Figs. 9 and 10. These trajectories are qualitatively very similar to the case when there is only a power limit, except that the torque constraint becomes active at low rotational speeds of the turbocharger.

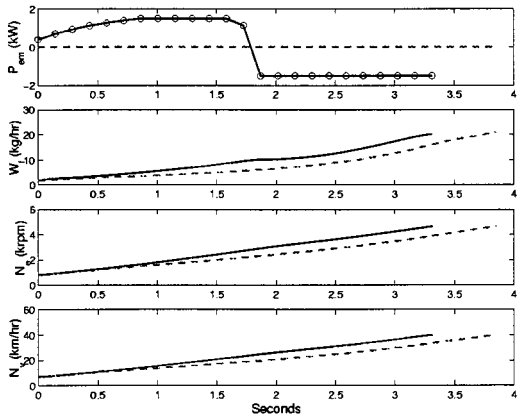

Fig. 9. Comparison of TPAS (solid) and conventional vehicle (dashed) for the first gear acceleration with torque constraint. Trajectories of P_{em}, W_f, N_e, N_v.

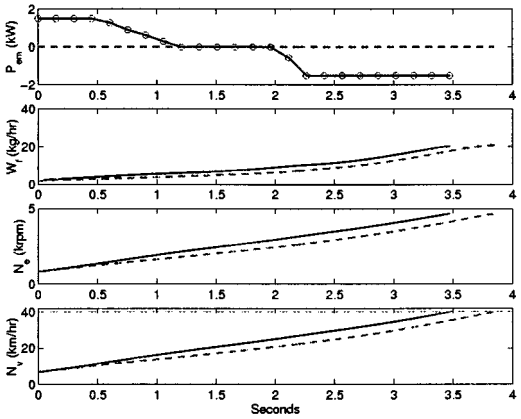

Fig. 11. Comparison of TPAS (solid) and conventional vehicle (dashed) for the first gear acceleration. The effect of TPAS efficiencies is included. Trajectories of P_{em}, W_f, N_e, N_v.

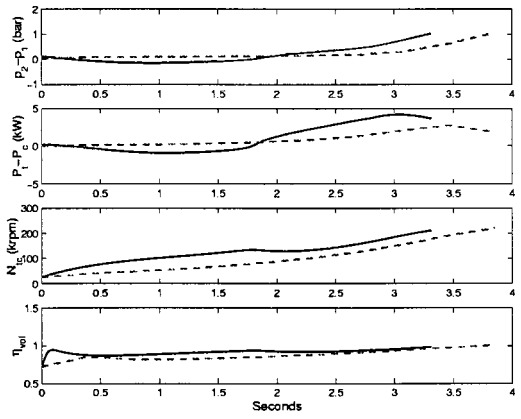

Fig. 10. Comparison of TPAS (solid) and conventional vehicle (dashed) for the first gear acceleration with torque constraint. Trajectories of $p_2 - p_1$, $P_t - P_c$, N_{tc}, η_{vol}.

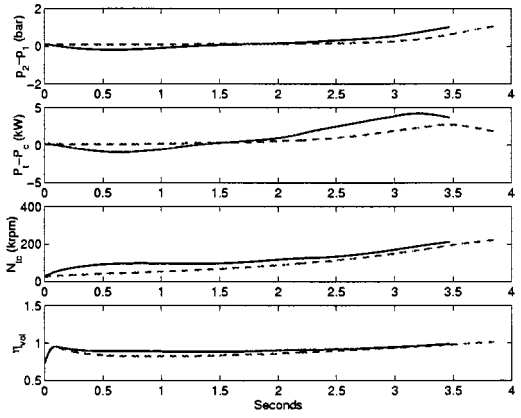

Fig. 12. Comparison of TPAS (solid) and conventional vehicle (dashed) for the third gear acceleration. The effect of TPAS efficiencies is included. Trajectories of $p_2 - p_1$, $P_t - P_c$, N_{tc}, η_{vol}.

D. Effect of TPAS Efficiency

To study the effect of losses we introduce a motoring efficiency, q_m, and a regenerating efficiency, q_g. The power applied to the turbocharger shaft or absorbed from the turbocharger shaft is P_{em}. If $P_{em} \geq 0$ then the power actually consumed from the energy storage (such as a battery) is P_{em}/q_m. If $P_{em} \leq 0$ then the power that can be put into the storage for future use is $q_g \cdot P_{em}$. Based on the preliminary information about the TPAS, the following values for the efficiencies have been assumed: $q_m = 0.9$ and $q_g = 0.7$. We have optimized the time for the first gear acceleration to 40 km/h subject to the maximum TPAS power limit of 1.5 kW and that all energy taken by the TPAS from the energy storage is regenerated back by the end of the acceleration. The minimum acceleration time was 3.47 s and the fuel consumption was 8.70 g. This is 1.64% deterioration in fuel consumption and 6.12% deterioration in acceleration time as compared to the ideal case (see Table I). The acceleration time and the fuel consumption are still better than for the case of the conventional vehicle. Figs. 11 and 12 show the optimized trajectories. Note that for a portion of time, $P_{em} = 0$. We can easily repeat the optimization for a range of values for q_m and q_g, to determine the acceptable range that meets our performance targets.

The evaluation of sensitivity to the turbine mechanical efficiency, η_m, (that may be different for the actual TPAS turbine as compared to the conventional vehicle turbine) can be done similarly to the evaluation of the sensitivity to motoring and regenerating efficiencies. In this way appropriate subsystem level requirements for this parameter can be also defined.

V. Implication for On-Line Controller Design

In intelligent transportation systems vehicles are expected to have necessary information and computing power to fully implement the optimal control scheme described so far. However, in conventional transportation applications an on-line controller is based only on the current values of the engine variables. Moreover, we cannot typically assume exact knowledge of future driver demand profile. In these cases, the development of an on-line controller is not a straightforward task. Although the focus of the paper is to generate optimal trajectories and assess potential benefits of the new device, the study of the optimal trajectories reveals important information for the design and gain tuning of an on-line feedback controller. Namely, the optimal pattern requires supplemental energy addition to the turbocharger shaft during the initial phase of the acceleration and energy regeneration during the final phase of the acceleration.

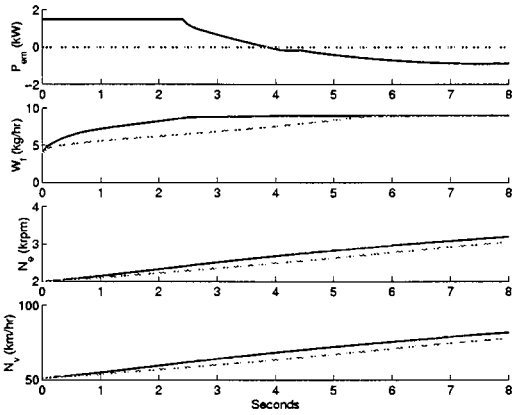

Fig. 13. Comparison of TPAS vehicle with an on-line controller (solid) and conventional vehicle (dashed) for the third gear acceleration. Trajectories of P_{em}, W_f, N_e, N_v.

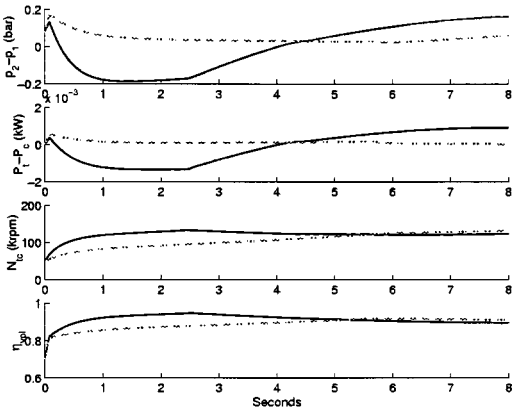

Fig. 14. Comparison of TPAS vehicle with an on-line controller (solid) and conventional vehicle (dashed) for the third gear acceleration. Trajectories of $p_2 - p_1$, $P_t - P_c$, N_{tc}, η_{vol}.

The control system would interpret the driver's pedal command as a request for a certain fueling rate, $W_{f,req}$. Based on the available air, the control system would then calculate the maximum admissible fueling rate, $W_{f,\max}$ under the no visible smoke constraint. If $W_{f,\max} < W_{f,req}$ then the engine would be fueling at a limited fueling rate, $W_{f,\max}$. We may judge that the acceleration is in its initial phase relative to the driver's intentions when the difference $W_{f,req} - W_{f,\max}$ is large positive and it is in the final phase of the acceleration when this difference is small or less than zero. It is relatively easy to setup a control scheme that sets the power demand from TPAS according to the difference $W_{f,req} - W_{f,\max}$ and the difference $E_{em} - E_{em,req}$ where $E_{em,req}$ is the desired energy level in the energy storage. For example, we evaluated in simulations the following scheme:

$$P_{em} = -\kappa_1(E_{em} - E_{em,req}) \cdot \max\{W_{f,\max} - W_{f,req},\, a\} + \kappa_2(W_{f,req} - W_f) \tag{48}$$

where $\kappa_1 > 0$, $\kappa_2 > 0$ are gains and $a \geq 0$ is a parameter. Note that the controller allows for a more aggressive regeneration of energy when $W_{f,\max} > W_{f,req}$.

Simulation results for the above scheme are shown in Figs. 13–15. The acceleration is in the third gear with constant

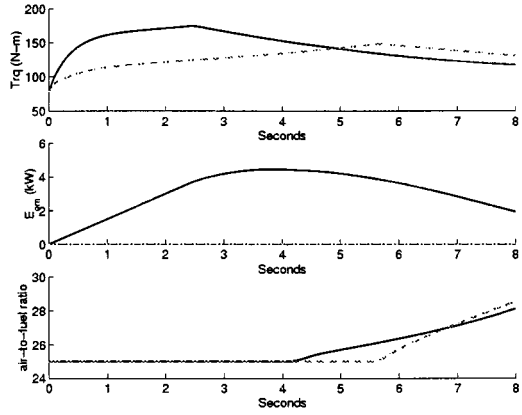

Fig. 15. Comparison of TPAS vehicle with an on-line controller (solid) and conventional vehicle (dashed) for the third gear acceleration. Trajectories of τ, E_{em}, (A/F).

$W_{f,req} = 9$ kg/h and with $E_{em,req} = 0$. There is an initial step change in the fueling rate from 1 kg/h to about 4 kg/h due to a sufficient amount of air already available in the engine intake manifold to support this increase in the engine fueling rate. The step change in W_f leads to an initially similar looking responses of the engine torque and of the manifold pressure difference $p_2 - p_1$ for both cases with and without the TPAS. The action of the TPAS is evident in the engine responses after this initial phase of 0.2 s. It results in the increased airflow to the engine and, hence, enables the increased delivery of fuel to the engine. It also results in a smaller manifold pressure difference $p_2 - p_1$ and reduced pumping losses. These two factors contribute to a much faster engine torque response with the TPAS and a smaller turbo-lag. When the difference $W_{f,req} - W_f$ is sufficiently reduced the controller starts to gradually regenerate the energy. The action of this controller should not be very aggressive to avoid a significant drop in the engine torque. Hence, the regenerative action extends over a sufficiently large time period as the net energy consumed by the TPAS, E_{em}, asymptotically approaches zero.

VI. Conclusion

In this paper we demonstrated how the optimal control-based analysis can be very useful in studying feasibility and cost/benefit trade-off for an automotive hardware component. This analysis is particularly important early on in the new powertrain design stage where it enables the right decisions to be made about the system hardware configuration. The analysis also leads to specification of subsystem level requirements and provides clues to the structure and implementation of the operating policy and control algorithms.

Appendix A
Gradient Calculation

The model is of the form

$$\frac{dx}{d\sigma} = TF(x(\sigma),\, u(\sigma)), \qquad 0 \leq \sigma \leq 1, \quad x(0) = x^0 \tag{49}$$

$$u(\sigma) = \sum_{i=0}^{n} \alpha_i \phi_i(\sigma). \tag{50}$$

Suppose we have a function g of the final state $x(1)$. We wish to determine its partial derivatives $(\partial g(x(1))/\partial \alpha_i)$, $i = 0, \ldots, n$, $(\partial g(x(1))/\partial T)$.

The adjoint equations have the form

$$\frac{dp}{d\sigma} = -T\left(\frac{\partial F}{\partial x}(x(\sigma), u(\sigma)\right)^T p \tag{51}$$

$$p(1) = \frac{\partial g}{\partial x}(x(1)). \tag{52}$$

The partial derivatives are then given by the expressions

$$\frac{\partial g(x(1))}{\partial \alpha_i} = T\int_0^1 \frac{\partial F}{\partial u}(x(\sigma), u(\sigma)) \cdot \phi_i(\sigma) \cdot p(\sigma)\, d\sigma, \quad i = 0, \ldots, n$$

$$\frac{\partial g(x(1))}{\partial T} = \int_0^1 p^T(\sigma) F(x(\sigma), u(\sigma))\, d\sigma$$

where $x(\sigma)$ is the solution of (49) and (50) in forward time; $p(\sigma)$ is the solution of (51) and (52) in backward time.

The derivation of these formulas follows by considering the perturbations $T \to T+\delta T, u \to u+\delta u$, where $\delta u = \sum_{i=0}^{n} \delta\alpha_i \cdot \phi_i$ and determining, to the first order, the resulting change in δy, where $y = g(x(1))$.

REFERENCES

[1] V. N. Afanas'ev, V. B. Kolmanovskii, and V. R. Nosov, *Mathematical Theory of Control Systems Design*. Boston, MA: Kluwer, 1996.

[2] M. Athans and P. L. Falb, *Optimal Control: An Introduction to the Theory and Its Applications*. New York: McGraw-Hill, 1966.

[3] "Turbo 2000: Turbocharging solutions for the next century," *Engine Technol. Int.*, no. 2/98, p. 49.

[4] A. E. Bryson, *Dynamic Optimization*. Reading, MA: Addison Wesley Longman, 1999.

[5] M. A. Gottschalk, "High-speed motor and drive target next-generation fuel cells," *Design News*, Oct. 20, 1997.

[6] M. Kao and J. J. Moskwa, "Turbocharged diesel engine modeling for nonlinear engine control and estimation," *ASME J. Dyn. Syst., Measurement, Contr.*, vol. 117, 1995.

[7] I. Kolmanovsky, P. Moraal, M. van Nieuwstadt, and A. Stefanopoulou, "Issues in modeling and control of variable geometry turbocharged engines," in *Systems Modeling and Optimization, Proc. of the 18th IFIP TC7 Conference (July 1997)*, CRC Research Notes in Mathematics, M. P. Polis, A. L. Dontchev, P. Kall, I. Lasiecka, and A. W. Olbrot, Eds, 1999, pp. 436–445.

[8] I. Kolmanovsky, M. van Nieuwstadt, and P. Moraal, "Optimal control of variable geometry turbocharged diesel engines with exhaust gas recirculation," in *Proc. ASME Dyn. Syst. Contr. Division 1999 ASME Int. Mech. Eng. Congr. Exposition*, vol. DSC-67, pp. 265–273.

[9] H. W. Knobloch, *Higher Order Necessary Conditions in Optimal Control Theory*. New York: Springer-Verlag, 1981.

[10] R. R. Lundstrom, "A comparison of transient vehicle performance using a fixed geometry, wastegated turbocharger and a variable geometry turbocharger," in *SAE paper 860 104*.

[11] D. Page, "Optimization of the air-fuel ratio for improved engine performance and reduced emissions," in *SAE paper 961 714*, 1996.

Ilya V. Kolmanovsky (S'94–M'95) studied as an undergraduate at Moscow Aviation Institute in Russia. He received the M.S. and Ph.D. degrees in aerospace engineering in 1993 and 1995 and the M.A. degree in mathematics in 1995 from the University of Michigan, Ann Arbor.

He is presently with Ford Research Laboratory in Dearborn, MI, conducting research on modeling, analysis, optimization, and control strategy development for advanced technology gasoline and diesel engine systems.

Anna G. Stefanopoulou (S'93–M'96) received the Diploma degree from the National Technical University of Athens, Greece, in 1991 and the M.S. degree in naval architecture and marine engineering and the M.S. and Ph.D. degrees in electrical engineering and computer science from the University of Michigan, Ann Arbor, in 1992, 1994, and 1996, respectively.

She was an Assistant Professor at the University of California, Santa Barbara, and a Technical Specialist at Ford Motor Company. She is presently an Associate Professor at the Mechanical Engineering Department at the University of Michigan. Her research interests include transportation systems, powertrain modeling and control, multivariable feedback theory, and control architectures for industrial applications.

Dr. Stefanopoulou is Chair of the Transportation Panel in ASME DSCD and a recipient of a 1997 NSF CAREER award.